Resonant Raman scattering from F center in Cs halides

E. Mulazzi*
Department of Physics, Purdue University, West Lafayette, Indiana 47907
(Received 28 November 1978)

The theory for the resonant Raman scattering from the F center in Cs halides is presented. It is proved that new selection rules for the first-order polarized resonant Raman scattering from these systems are necessary because of the spin-orbit interaction in the excited electronic state. The evaluation of the first-order resonant Raman scattering is performed within resonant Raman scattering theory by including the spin-orbit interaction and the properties of the Γ_1^+, Γ_3^+, Γ_5^+ electron-phonon interaction.

I. INTRODUCTION

Recent experimental data on Raman scattering in resonance with the F band in alkali halides and cesium halides[1] have shown that the usual selection rules[2] for the Γ-symmetry phonons responsible for the first-order polarized Raman scattering are not valid under resonance conditions. In particular, it was found that each of the $[100]\rightarrow[100]$, $[110]\rightarrow[1\bar{1}0]$, and $[100]\rightarrow[010]$ polarized first-order scattering spectra is determined by the superposition of all three projected densities of phonon states $\rho(\Gamma,\omega^2)$ associated with phonons of Γ_1^+, Γ_3^+, and Γ_5^+ symmetry. These results are in contrast with the predictions of the usual selection rules[2] which state that only phonons of Γ_1^+ and Γ_3^+ symmetry contribute to the $[100]\rightarrow[100]$ spectrum, only phonons of Γ_3^+ symmetry contribute to the $[110]\rightarrow[1\bar{1}0]$ spectrum, and only phonons of Γ_5^+ symmetry contribute to the $[100]\rightarrow[010]$ spectrum. These changes in the selection rules had already been predicted in earlier work by the author (example 3 of Ref. 3). They were subsequently illustrated by the results of numerical calculations of Raman scattering cross sections in resonance with the F bands in CsF (Ref. 4) and in CsBr (Ref. 5) on the basis of the theory presented in detail in the present paper. In Ref. 4 the changes in the integrated intensity of the Raman scattering cross sections due to the new selection rules were demonstrated in a qualitative way on the basis of approximate forms for the projected photon densities of states. The changes of the Raman scattering cross sections in resonance with the F band in CsBr were presented in Ref. 5 in which accurate projected densities of phonon states were used.

In Refs. 4 and 5 it was shown that the breakdown of the usual selection rules for first-order polarized Raman scattering under resonance conditions is caused by the spin-orbit interaction in the first excited state of the F center and by the spin-degenerate ground state. In fact, this effect can be observed when the frequency of the incident laser light is in resonance with a dipole active electronic transition from a spin-degenerate ground state to an excited state in which the spin-orbit interaction is nonvanishing. The F center in alkaki halides provides a good test for this effect since its ground state is spin degenerate and the spin-orbit interaction is nonvanishing in its first excited states. Moreover, in the first electronic excited state of the F center in the alkali and cesium halides, the electron-phonon interactions transforming according to the Γ_1^+, Γ_3^+, and Γ_5^+ irreducible representations have different strengths, as can be inferred from the different shapes of the F bands, e.g., of CsBr (Ref. 5) and CsF.[4] This property makes the study of the F-center resonant Raman scattering interesting because the contributions of $\rho(\Gamma_1^+,\omega^2)$, $\rho(\Gamma_3^+,\omega^2)$, and $\rho(\Gamma_5^+,\omega^2)$ in all three polarized spectra also depend on the strengths of the electron-phonon interaction transforming as Γ_1^+, Γ_3^+, and Γ_5^+, as will be shown in the present paper. Therefore, the new selection rules for Raman scattering in resonance with the different F bands can be tested also by the change in the relative contributions of $\rho(\Gamma_1^+,\omega^2)$, $\rho(\Gamma_3^+,\omega^2)$, and $\rho(\Gamma_5^+,\omega^2)$ to all three polarized spectra. More precisely, since the Γ_1^+ electron-phonon interaction is usually the strongest one in the first excited state of the F center and is responsible for the broad shape of the absorption band, the breakdown of the selection rules is confirmed by the appearance of the projected density of phonon states $\rho(\Gamma_1^+,\omega^2)$ in all the first-order polarized spectra. [This is observed, for example, in the resonant Raman scattering from the F center in KI (Ref. 1) and CsBr.[1,5]] On the other hand, when the dynamical Jahn-Teller effect due to the electron-phonon interactions of Γ_3^+ and Γ_5^+ symmetry is strong enough to produce structure in the absorption band, then the projected densities of phonon states $\rho(\Gamma_3^+,\omega^2)$ and $\rho(\Gamma_5^+,\omega^2)$ can also play important roles in determining the shapes of all first-order polarized scattering spectra [as can be seen[1] in the resonant Raman scattering from the F center in

 © 1980 The American Physical Society

CsF (Ref. 1)].

A good test of the theory presented in this paper can be made by comparing the calculated first-order polarized resonant Raman spectra for the F center in CsBr and CsF with the experimental data. That is another of the aims of this paper.

In this paper (i) we present the theory of Raman scattering in resonance with the F band in the cesium halides, (ii) we apply this theory to the evaluation of the differential Raman cross sections in resonance with the F band in CsF and we compare these results with the experimental data,[1] and (iii) we compare these latter results with those obtained previously for CsBr.[5]

In Sec. II we give the selection rules for Raman scattering from a defect in a crystal characterized by ground and excited states transforming as Γ_6^+ and $\Gamma_8^- + \Gamma_6^-$, respectively, taking into account the electron-phonon interactions of Γ_1^+, Γ_3^+, Γ_5^+ symmetry. In Sec. III we present theoretical expressions for the first-order resonant Raman cross sections for the $[100] \rightarrow [100]$, $[110] \rightarrow [1\bar{1}0]$, and $[100] \rightarrow [010]$ polarized scatterings. In Sec. IV we compare the theoretical evaluations of the first-order Raman scattering cross sections in resonance with the F band in CsF with the experimental data[1] and we discuss these results with those obtained for CsBr.[5] In Sec. V we present our conclusions. The starting point of the theory we give here is the resonant Raman-scattering response function derived in Ref. 6 that describes the scattering processes when the laser light frequency is in resonance with a $\Gamma_1^+ \rightarrow \Gamma_4^-$ optical transition. In that case, the new scattering selection rules arise solely as a result of the dynamical Jahn-Teller effect. In contrast, in the present case the effect is due mainly to the spin-orbit interaction,[4,5] which considerably modifies the resonant Raman response function. Moreover, the Γ_1^+, Γ_3^+, and Γ_5^+ electron-phonon interactions, as we have shown in Ref. 7, must be treated differently than for the triply degenerate excited state of Ref. 6.

The evaluations of the time ordering of the electron-phonon interactions and the phonon propagators in the resonant Raman-scattering response function are performed in the independent-ordering approximation (IOA), as was done for the absorption band-shape[7,5,4] problem. Using the same theoretical approach for evaluating both the absorption band shape and the first-order Raman scattering cross section, as we have already done for the F center in CsBr, provides better information about the electron-phonon coupling and the densities of phonon states than if different approaches are used in the two calculations. Moreover, if one applies the theory presented here for the F center in Cs halides to a system in which both the ground and the excited electronic states transform according to double group representations, one obtains the same new selection rules. In other words, these selection rules apply in all cases in which the spin degeneracy and the spin-orbit interaction actively enter in determining the properties of the ground and the excited states that are connected through the electric dipole moment. For instance, they can be observed in the case of resonant Raman scattering from the layered $3d$ metal halides[8] where the above conditions for the ground and the excited states apply. An additional consequence of the selection rules discussed in the present paper is that the antisymmetric component (Γ_4^+) of the Raman tensor is dominant when the incident laser frequency is in resonance with the electronic transition that connects spin-degenerate states. This effect has been observed in resonant Raman scattering from rare-earth chalcogenides[9] with spin-degenerate ground states and for which the spin-orbit interaction in the excited states plays an important role in the scattering processes.

II. SELECTION RULES

In this section, we derive selection rules for phonons that are involved in the scattering from a system whose electronic ground state transforms as Γ_6^+. The starting point of this analysis is taken from the work presented in Ref. 10 for the off-resonant vibrational Raman scattering from impurities characterized by the dynamical Jahn-Teller effect of the interactions between the electronically degenerate ground state and the lattice vibrations. In the problem of interest in the present paper, the physical situation is different from that considered in Ref. 10, since here there is no dynamical Jahn-Teller effect in the ground state and the new selection rules are determined by the spin degeneracy in the ground state and by the spin-orbit interaction in the excited state. Moreover, as we will discuss later, the new selection rules become important only when the incident light frequency is in resonance with the optical transition $\Gamma_6^+ \rightarrow \Gamma_8^- + \Gamma_6^-$. Since the ground state is a Γ_6^+ doublet and the electric-dipole-moment operator in O_h symmetry transforms like Γ_4^-, the excited states connected to the ground state via the electronic transition must transform as $\Gamma_8^- + \Gamma_6^-$.

In fact,

$$\Gamma_6^+ \otimes \Gamma_4^- \in \Gamma_8^- + \Gamma_6^- . \tag{1}$$

Moreover,

$$[(\Gamma_8^- + \Gamma_6^-)^2]_s \in \Gamma_1^+ + \Gamma_3^+ + \Gamma_5^+ . \tag{2}$$

Then the electron-phonon interactions that create the phonons involved in the scattering transform according to Γ_1^+, Γ_3^+, and Γ_5^+. Only the symmetric part of the direct product $(\Gamma_8^- + \Gamma_6^-) \otimes (\Gamma_8^- + \Gamma_6^-)$ in Eq. (2) must be considered, since the electron-phonon interactions acting in a particular electronic state (in this case $\Gamma_8^- + \Gamma_6^-$) are always symmetric.[11] Then by considering Eqs. (1) and (2) and the irreducible representations of the reduction of $(\Gamma_4^-)^2$ that enter into the different polarized scatterings, as has been shown in Ref. 3 and Eqs. (12) and (13) of Ref. 10, one finds the following selection rules:

$$
\begin{aligned}
&[(\Gamma_6^+)^2 \otimes (\Gamma_1^+ + \Gamma_3^+)]_s = \Gamma_1^+ + \Gamma_3^+ + \Gamma_5^+, \\
&\quad \hat{n}^L \| [100], \ \hat{n}^R \| [100] \\
&[(\Gamma_6^+)^2 \otimes (\Gamma_3^+ + \Gamma_4^+)]_s = \Gamma_1^+ + \Gamma_3^+ + \Gamma_5^+, \\
&\quad \hat{n}^L \| [110], \ \hat{n}^R \| [1\bar{1}0] \\
&[(\Gamma_6^+)^2 \otimes (\Gamma_4^+ + \Gamma_5^+)]_s = \Gamma_1^+ + \Gamma_3^+ + \Gamma_5^+, \\
&\quad \hat{n}^L \| [100], \ \hat{n}^R \| [010]
\end{aligned}
\tag{3}
$$

where $\hat{n}^L$ and $\hat{n}^R$ are the incident and scattered light polarization vectors.

Note that the excited states that transform according to Γ_8^- and Γ_6^- are implicitly included in Eq. (3) if one makes use of Eq. (1). [See, for instance, Eqs. (8) and (9) of Ref. 10.] Equation (3) states that the densities of phonon states $\rho(\Gamma_1^+, \omega^2)$, $\rho(\Gamma_3^+, \omega^2)$, and $\rho(\Gamma_5^+, \omega^2)$ together contribute to the first-order Raman scattering for all the listed polarization geometries. Moreover, since $(\Gamma_6^+)^2 = \Gamma_1^+ + \Gamma_4^+$, the Γ_4^+ component of the Raman tensor plays a very important role in determining the new selection rules for the phonons involved in the $[110] \rightarrow [1\bar{1}0]$ and $[100] \rightarrow [010]$ polarized scattering processes [see Eq. (3)]. For instance, from Eq. (3) it is straightforward to show that $\rho(\Gamma_1^+, \omega^2)$ contributes to the above-mentioned first-order polarized scattering spectra only because the Γ_4^+ Raman tensor component must be considered in these polarized scattering processes. Furthermore, a very simple test that the Γ_4^+ Raman component is the dominant one in determining the $[110] \rightarrow [1\bar{1}0]$ and $[100] \rightarrow [010]$ polarized scatterings can be made whenever, for instance, the $\rho(\Gamma_1^+, \omega^2)$ contribution becomes the strongest one in these polarized scattering spectra. This point will be discussed in connection with the resonant Raman scattering from CsBr.[5] On the other hand, when the Jahn-Teller interactions (Γ_3^+, Γ_5^+) play an important role in the excited states $(\Gamma_6^- + \Gamma_8^-)$, the Γ_4^+ component of the Raman tensor enhances the contributions of $\rho(\Gamma_3^+, \omega^2)$ and $\rho(\Gamma_5^+, \omega^2)$ in the $[100] \rightarrow [010]$ and $[110] \rightarrow [1\bar{1}0]$ polarized scatterings, respectively. This point will be discussed in connection with the resonant Raman scattering from CsF.

Therefore, employing Eq. (3), the differential first-order Raman cross section at $T = 0$ K can be written in the following way for all the incident and scattered light polarization geometries[3]:

$$
\begin{aligned}
\frac{d^2\sigma}{d\Omega\, d\omega} \propto\ & a_1(\hat{n}^L, \hat{n}^R, \omega_L)\rho(\Gamma_1^+, \omega^2) + a_3(\hat{n}^L, \hat{n}^R, \omega_L)\rho(\Gamma_3^+, \omega^2) \\
& + a_5(\hat{n}^L, \hat{n}^R, \omega_L)\rho(\Gamma_5^+, \omega^2), \quad i = 1, 3, 5
\end{aligned}
\tag{4}
$$

where the coefficients $a_i(\hat{n}^L, \hat{n}^R, \omega_L)$ depend on the different polarization geometries, the laser light frequency ω_L, the electron-phonon interaction coupling, and the oscillator strength for the electronic transition. The aim of this paper is to give the theory for evaluating the $a_i(\hat{n}^L, \hat{n}^R, \omega_L)$ coefficients when the laser frequency is in resonance with the transition $\Gamma_6^+ \rightarrow \Gamma_8^- + \Gamma_6^-$. Nevertheless, it is useful to show relations for the differential Raman cross sections for the off-resonance condition, when only one excited state transforming as $\Gamma_8^- + \Gamma_6^-$ is considered. We do this in order to compare the off-resonance case with the results we will present later for the in-resonance case.

By using Eq. (7) of Ref. 10 and the matrix representations of the electron-phonon interactions in the excited states $\Gamma_8^- + \Gamma_6^-$ and of the electric dipole moments for the $\Gamma_6^+ \rightarrow \Gamma_8^- + \Gamma_6^-$ transition given in Ref. 7 [Eqs. (6)–(9) and (A4)], we find

$$
a_1(\hat{n}^L, \hat{n}^R, \omega_L) = \tau(\omega_L)\tfrac{1}{9}C^2(\Gamma_1^+) \times \begin{cases} |S_{22}(\omega_L) + 2S_{11}(\omega_L)|^2, & [100] \rightarrow [100] \\ |S_{11}(\omega_L) - S_{22}(\omega_L)|^2, & [110] \rightarrow [1\bar{1}0] \\ |S_{11}(\omega_L) - S_{22}(\omega_L)|^2, & [100] \rightarrow [010] \end{cases} \tag{5a}
$$

$$
a_3(\hat{n}^L, \hat{n}^R, \omega_L) = \tau(\omega_L)\tfrac{1}{9}C^2(\Gamma_3^+) \times \begin{cases} 4|S_{11}(\omega_L) + S_{12}(\omega_L) + S_{21}(\omega_L)|^2, & [100] \rightarrow [100] \\ 3|S_{11}(\omega_L) + S_{12}(\omega_L) + S_{21}(\omega_L)|^2 + |2S_{11}(\omega_L) - S_{12}(\omega_L) - S_{21}(\omega_L)|^2, & [110] \rightarrow [1\bar{1}0] \\ |S_{11}(\omega_L) + S_{12}(\omega_L) - 2S_{21}(\omega_L)|^2 + 3|S_{11}(\omega_L) - S_{12}(\omega_L)|^2, & [100] \rightarrow [010] \end{cases} \tag{5b}
$$

$$a_5(\vec{n}^L,\vec{n}^R,\omega_L)=\tau(\omega_L)C^2(\Gamma_5^+)\tfrac{1}{3}\times\begin{cases}2\,|S_{12}(\omega_L)-S_{21}(\omega_L)|^2, & [100]\to[100]\\ 2\,|S_{12}(\omega_L)-S_{21}(\omega_L)|^2, & [100]\to[1\bar{1}0]\\ |S_{11}(\omega_L)+S_{21}(\omega_L)+S_{12}(\omega_L)|^2+|S_{11}(\omega_L)-S_{21}(\omega_L)|^2+|S_{11}(\omega_L)-S_{12}(\omega_L)|^2, & [100]\to[010]\end{cases}\tag{5c}$$

where

$$\tau(\omega_L)=\frac{(M_{sp}^0)^4}{2\pi}p\left(\frac{\omega_L}{c}\right)^4,\tag{6}$$

p is the concentration of defects in the crystal and M_{sp}^0 is given in Eq. (A4) of Ref. 7. The $C(\Gamma_i^+)$ are the electron-phonon interaction couplings.[12] The $S_{\alpha\alpha'}(\omega_L)$ functions for the off-resonance condition are given by

$$S_{\alpha\alpha'}(\omega_L)=\left(\frac{1}{(E_\alpha-\omega_L-\omega)(E_{\alpha'}-\omega_L)}+\frac{1}{(E_\alpha+\omega_L-\omega)(E_{\alpha'}+\omega_L)}\right),\quad \alpha,\alpha'=1,2\tag{7}$$

where ω is the phonon frequency corresponding to the Stokes frequency shift and

$$E_1=E_0+\lambda,\quad E_2=E_0-\tfrac{1}{2}\lambda\,.\tag{8}$$

E_0 is the electronic excited-state energy evaluated without the spin-orbit interaction and λ is the spin-orbit constant. When the lifetime of the electronic state must be considered, one must make the replacement

$$E_\alpha\to E_\alpha-i\gamma\,,\tag{9}$$

where γ is the inverse of the lifetime of the excited states Γ_8^- and Γ_6^-. For the case of the F center in Cs halides and alkali halides, γ has a small and usually negligible value.

The derivation for the more general case where m sets of excited states transforming as $\Gamma_8^-+\Gamma_6^-$ are considered is straightforward if one uses, for instance, the formula given in Ref. 10 and, in addition, takes into account the electronic phonon interactions transforming as Γ_3^+ and Γ_5^+, which mix the different m sets of states $\Gamma_8^-+\Gamma_6^-$.

It is easy to derive from Eqs. (7) that $S_{12}(\omega_L)=S_{21}(\omega_L)$ when

$$\frac{\omega\,|\lambda\,|}{(\omega_L-E_1)^2(\omega_L-E_2)^2}\tag{10a}$$

is negligible and $S_{11}(\omega_L)=S_{22}(\omega_L)$ when

$$\frac{\omega_L\,|\lambda\,|}{(\omega_L-E_1)^2(\omega_L-E_2)^2}\tag{10b}$$

is negligible. For the off-resonance condition, when both the quantities of Eqs. (10a) and (10b) are negligible and $S_{11}(\omega_L)=S_{22}(\omega_L)=S_{12}(\omega_L)=S_{21}(\omega_L)$, the usual selection rules[2] become valid as can be seen from Eqs. (4), (5), and (7). The new selection rules begin to be valid when the laser frequency ω_L is near the resonance condition; i.e., ω_L is in a frequency region below the absorption band spectrum and both the quantities given in Eqs. (10a) and (10b) are not negligible. The intensity of the new scattering processes reaches a maximum when the laser light is in resonance with the absorption band due to the transition $\Gamma_6^+\to\Gamma_8^-+\Gamma_6^-$. Moreover, when the laser light ω_L is in resonance with the absorption band, as in the case of the F band in Cs halides, Eqs. (7) become incorrect even if the modification given in Eq. (9) is introduced. In fact, for the in-resonance condition, the absorption band shape becomes crucial in determining the Raman cross-section intensities. Then in the case of broadened bands with possible Jahn-Teller structure, as for the F band in Cs halides, the use of a fictitious value of γ for simulating the band-shape broadening due to the correlation of many phonon processes may be incorrect. Furthermore, by using Eq. (7), the consequences of the dynamical Jahn-Teller effect on the intensity of the Raman cross sections are completely neglected. More important, in resonance the Raman cross sections depend on the square of the modulus of both the real and imaginary parts of the response function of the system considered, as will be shown in the next section.

III. RESONANCE RAMAN-SCATTERING CROSS SECTIONS

We give in this section the theory for evaluating the differential cross section for defect-induced Raman scattering in resonance with the transition $\Gamma_6^+\to\Gamma_8^-+\Gamma_6^-$, with particular attention to the case of the F center in Cs halides. We use as a starting point the theory of Ref. 6, which takes into account the dynamical Jahn-Teller effect in the degenerate excited states. We note that in the case under consideration in the present paper, the spin-orbit interaction plays an important role

together with the electron-phonon interactions in determining the properties of the resonant Raman-scattering differential cross sections. We use all the notations and symbols introduced in Ref. 7 for the absorption process due to the $\Gamma_6^+ \rightarrow \Gamma_8^- + \Gamma_6^-$ transition:

$$\frac{d^2\sigma}{d\omega\, d\Omega} \propto \frac{p}{(2\pi)^2}\left(\frac{\omega_L}{c}\right)^4 \int_{-\infty}^{+\infty} d\mu\, e^{i\omega\mu} \int_0^\infty dt \int_0^\infty dt'\, e^{-i\omega_L(t-t')} e^{-\gamma(t+t')} S(t,t',\mu)\,, \tag{11}$$

$$S(t,t',\mu) = \mathrm{Tr}\langle T_{tt'}\{[R_{(s')s'}(t')]^*[R_{(s+\mu+t'-t)s}(t)]\}\rangle_{B,\mathrm{conn}}\,, \tag{12}$$

where

$$R_{(s')s'}(t') = \sum_{\nu\nu'} n_\nu^L \sum_{\alpha=1}^{2} \sum_{m'} \sum_{jj'} e^{tB_\alpha^* t}\left\{M_{\nu,j'm}^{(\alpha)}(t') a_{j'}\left[\exp\left(i\int_0^{t'} H_{ep}^{(\alpha)}(s')ds'\right)\right]_{j'j} a_j^\dagger M_{\nu' jm'}^{(\alpha)}(0)\right\} n_{\nu'}^R\,. \tag{13}$$

$R_{(s+\mu+t'-t)s}(t)$ has an expression analogous to that given in Eq. (13). $\nu,\nu' = x,y,z$; when $\alpha=1$, $j=1$–4; when $\alpha=2$, $j=5,6$ as in Ref. 7. μ is the time variable for the Raman-scattering processes; $t(t')$ is the time variable for the processes induced by the electronic transition from the ground state (excited state) to the excited state (ground state). $T_{tt'}$ is the time-ordering operator for the processes in t and t'. All the operators in Eqs. (12) and (13) evolve in time in the interaction representation when time evolution is indicated. Note that the $M_{\nu,jm}^{(\alpha)}$ appearing in Eq. (13) have the same expression as $M_\nu^{(\alpha)}(jm;\{u\})$, the electric-dipole-moment operators that are dependent on the lattice displacement given in Eq. (11c) of Ref. 7. Also in Ref. 7, the expressions of E_α^* are given. In the evaluation of the function $S(t,t',\mu)$, with the inclusion of the properties of the electron-phonon interactions Γ_1^+, Γ_3^+, Γ_5^+ in the excited states Γ_6^- and Γ_8^-, we follow the same mathematical approach as used in Ref. 7 for the evaluation of the absorption band. Then the evaluations of $S(t,t',\mu)$ are performed in the IOA by considering only the terms proportional to t^2 in the expansion of $\varphi(\Gamma,t)$ and $\varphi(\Gamma,t')$ [see Eq. (23) of Ref. 7].[13] In this way, we are able to evaluate for the in-resonance condition the functions $S_{\alpha\alpha'}(\omega_L)$ ($\alpha,\alpha' = 1,2$), which define the coefficients given in Eqs. (5) of the differential Raman cross section in Eq. (4). These $S_{\alpha\alpha'}(\omega_L)$ functions, in the limit that γ is negligible, are given by

$$S_{\alpha\alpha}(\omega_L) = [S_\alpha(E_\alpha - \omega - \omega_L) - S_\alpha(E_\alpha - \omega_L)]/\omega\,, \tag{14}$$

$$S_{\alpha\alpha'}(\omega_L) = \pm[S_\alpha(E_\alpha - \omega - \omega_L) - S_{\alpha'}(E_{\alpha'} - \omega_L)] \times [2/(3|\lambda| \pm 2\omega)]\,, \quad \alpha \neq \alpha' = 1,2 \tag{15}$$

where the + signs apply for $\alpha=1$, $\alpha'=2$, and the − signs for $\alpha=2$, $\alpha'=1$ in Eq. (15). Here, we have

$$S_\alpha(\xi) = \Phi_\alpha(\xi) + i\theta_\alpha(\xi)\,, \tag{16}$$

$$\Phi_1(\xi) = \left(\frac{\pi}{2}\right)^{1/2} \frac{1}{N_1} A_1^4 \int_0^1 dx \frac{x^2}{\alpha(x)^{5/2}} G_1(\xi,x)\,, \tag{17}$$

$$\theta_1(\xi) = \frac{1}{N_1}\int_0^1 dx \frac{x^2}{\alpha(x)}\left(\theta_1^f(\xi,x) + \tfrac{2}{3}(\tfrac{4}{3}A_3 + 2A_5)\frac{1}{\lambda^2}\theta_1^f(\xi-\omega,x)\right), \tag{18}$$

$$\theta_1^f(\xi,x) = 3\xi \exp[-\xi^2/2\alpha(x)]\left({}_1F_1(\tfrac{1}{2};\tfrac{3}{2};\xi^2/2\alpha(x)) - \frac{4[\alpha(x)-A_1^2]}{\alpha(x)}\,{}_1F_1(-\tfrac{1}{2};\tfrac{3}{2};\xi^2/2\alpha(x)) + \frac{8}{3}\frac{[\alpha(x)-A_1^2]}{\alpha(x)^2}\,{}_1F_1(-\tfrac{3}{2};\tfrac{3}{2};\xi^2/2\alpha(x))\right), \tag{19}$$

$$\Phi_2(\xi) = \left(\frac{\pi}{2}\right)^{1/2} \frac{1}{A_1}\frac{1}{N_2} G_2(\xi)\,, \tag{20}$$

$$\theta_2(\xi) = (1/A_1N_2)\xi F_2(\xi)[{}_1F_1(\tfrac{1}{2},\tfrac{3}{2},\xi^2/2A_1^2) + (\xi-\bar{\omega})\tfrac{4}{3}(\tfrac{4}{3}A_3^2 + 2A_5^2)F_2(\xi-\bar{\omega})\,{}_1F_1(\tfrac{1}{2};\tfrac{3}{2};(\xi-\bar{\omega})^2/2A_1^2)]\,. \tag{21}$$

The functions $G_1(\xi, x)$, $G_2(\xi)$, and $F_2(\xi)$, the coefficients A_i and $\alpha(x)$, $\bar{\omega}$, and the normalization factors N_1 and N_2 are given in Ref. 7. ${}_1F_1(\frac{1}{2}n, \frac{1}{2}n', \xi^2)$ are hypergeometric functions. Then by substituting the expression for $S_{\alpha\alpha'}(\omega_L)$ given by Eqs. (14) and (15) into Eqs. (5), one can evaluate the resonant Raman-scattering cross section, Eq. (4).

We note that in the limit $|\xi/A_1| \gg 1$ and $|\xi/\alpha(x)| \gg 1$, it is possible to use the asymptotic expansion for the functions $S_\alpha(\xi)$ appearing in Eqs. (16)–(21), which then becomes

$$S_\alpha(\xi) = 1/\xi \,, \tag{22}$$

so that

$$S_{\alpha\alpha'}(\omega_L) = \frac{1}{(E_\alpha - \omega_L - \omega)(E_{\alpha'} - \omega_L)} \,, \quad \alpha, \alpha' = 1, 2 \,. \tag{23}$$

The expression for the functions $S_{\alpha\alpha'}(\omega_L)$ become equal to the first term of the expressions given in Eq. (7), which in this limit gives the more important contribution, the other term being always off-resonance and giving a negligible contribution with respect to the first term. Even if these last terms are included in the present calculations, the results do not change because the asymptotic expansion is always valid for $S_\alpha(\xi)$ when $\xi = \omega_L + E_\alpha - \omega$ or $\xi = \omega_L + E_\alpha$.

IV. DISCUSSION AND COMPARISON WITH EXPERIMENTAL DATA

We discuss here the results we have obtained with the theory presented in Sec. III for the polarized Raman-scattering spectra in resonance with the F band in CsF and comparisons with the available experimental data.[1] In addition, we compare these results with those previously obtained for CsBr (Ref. 5).

By following the method shown in Sec. III, it is possible to evaluate the absorption band shape and the resonant Raman-scattering cross section in a consistent way. In fact, the same functions and the same coefficients A_i determine the absorption band shape and the intensities for the different Raman-scattering processes as functions of ω_L [see Eqs. (17)–(21) of the present paper and Eqs. (42)–(45) of Ref. 7]. Moreover, the electron-phonon interactions and the projected perturbed densities of phonon states that define, when integrated, the coefficients A_i are the same ones that enter the differential Raman cross sections.

In general, the extent of the space around the defect that is important for the consideration of the electron-phonon interactions and the ion displacement correlations depends upon the extension of the excited-state wave functions compared with that of the ground state. If only the first excited state of the F center is important, it is a good approximation to include only the interactions between the electrons and the nearest-neighbor (NN) and next-nearest-neighbor (NNN) ion displacements. Then in all the cases,[5,7] where A_i coefficients are written as

$$A_i^2 = C_1^2(\Gamma_i)\left(\int_0^\infty \rho_{11}(\Gamma_i^+, \omega^2)d\omega + 2\alpha_i \int_0^\infty \rho_{12}(\Gamma_1^+, \omega^2)d\omega + \alpha_i^2 \int_0^\infty \rho_{22}(\Gamma_i^+, \omega^2)d\omega\right) , \tag{24}$$

with

$$\alpha_i = C_{22}(\Gamma_i^+)/C_{11}(\Gamma_i^+) \,, \tag{25}$$

the terms $C^2(\Gamma_i^+)\rho(\Gamma_i^+, \omega^2)$ in front of the $S_{\alpha\alpha'}(\omega_L)$ functions [see Eqs. (4) and (5)] must change in an analogous way as

$$C^2(\Gamma_i^+)\rho(\Gamma_i^+, \omega^2) \to C_{11}^2(\Gamma_i^+)[\rho_{11}(\Gamma_i^+, \omega^2) + 2\alpha_i\rho_{12}(\Gamma_i^+, \omega^2) + \alpha_i^2\rho_{22}(\Gamma_i^+, \omega^2)] \equiv C_{11}^2(\Gamma_i^+)R(\Gamma_i^+, \omega^2) \,, \tag{26}$$

where $R(\Gamma_i^+, \omega^2)$ is defined as the terms inside the square brackets.

For the rocksalt structure (CsF for instance),

$$C_{11}(\Gamma_i^+) = f_{11}(\Gamma_i^+)/\sqrt{M_1} \,, \quad C_{22}(\Gamma_i^+) = f_{22}(\Gamma_i^+)/\sqrt{M_2} \,, \tag{27}$$

where $f_{11}(\Gamma_i^+)$ and $f_{22}(\Gamma_i^+)$ are the coupling constants of the interaction forces between the electron and the NN and the NNN ion displacements, respectively; M_1 and M_2 are the relative NN and NNN ionic masses. $\rho_{11}(\Gamma_i^+, \omega^2)$ and $\rho_{22}(\Gamma_i^+, \omega^2)$ are the projected densities of phonon states determined by the autocorrelation of the NN displacements and the NNN displacements, respectively. The $\rho_{12}(\Gamma_i^+, \omega^2)$ are the perturbed projected densities of phonon states of the correlation between the NN and the NNN displacements. For the Cs halide structure see the discussion in Appendix B of Ref. 7 and in Ref. 5.

From the values of A_i obtained by fitting the experimental band shape one can evaluate the electron-phonon interaction couplings once the perturbed projected densities of phonon states $\rho_{ij}(\Gamma_i^+, \omega^2)$ are known. In fact, from Eqs. (24) and (26) one finds

$$C_{11}^2(\Gamma_i^+) = A_i^2\left(\int_0^\infty R(\Gamma_i^+, \omega^2)d\omega\right)^{-1} . \tag{28}$$

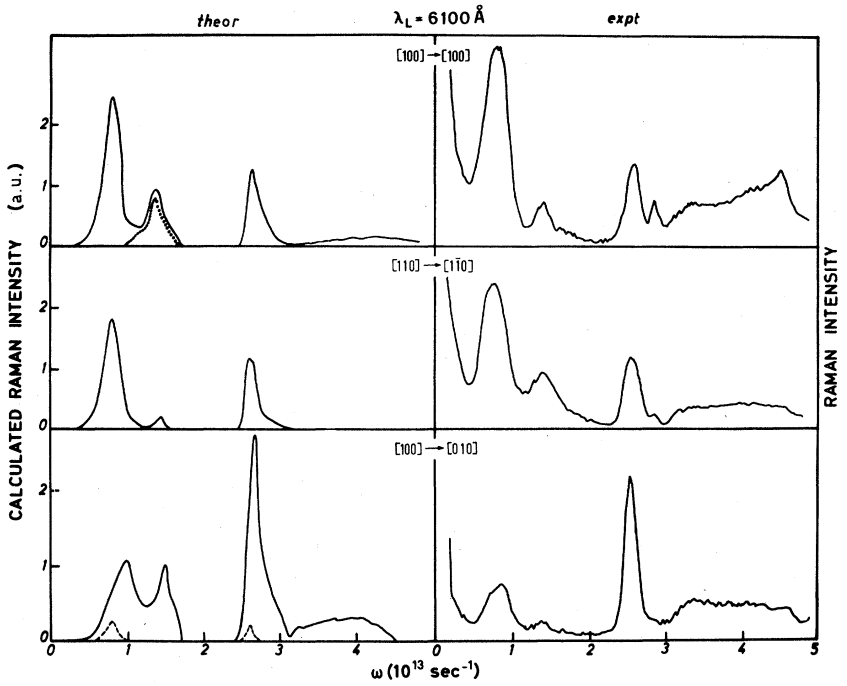

FIG. 1. On the left-hand side the theoretical differential first-order Raman cross sections for the indicated incident and scattered light polarizations and for $\lambda_L = 6100$ Å are shown. On the right-hand side the experimental data taken from Ref. 1 are shown for comparison. The significance of the different curves on the left-hand side is explained in the text.

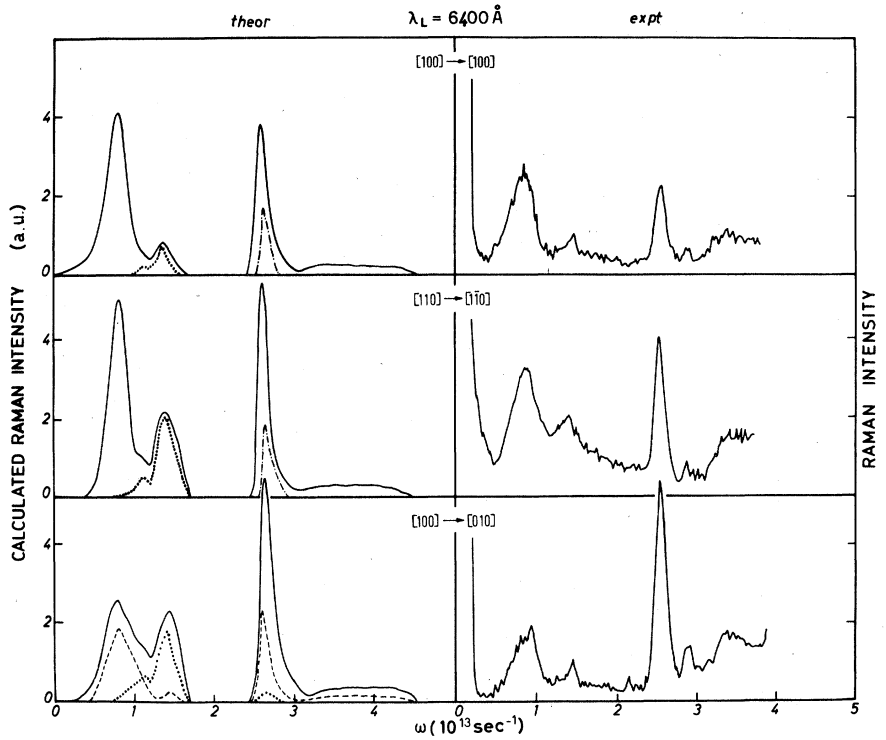

FIG. 2. Same as Fig. 1, for $\lambda_L = 6400$ Å.

Then Eq. (26) and consequently the terms in front of the $S_{\alpha\alpha'}(\omega_L)$ functions in Eqs. (5) become

$$A_i^2 R(\Gamma_i^+, \omega^2)\left(\int_0^\infty R(\Gamma_i^+, \omega^2) d\omega\right)^{-1}. \quad (29)$$

Then by using the method presented here, it is sufficient to know the A_i and the projected perturbed densities of phonon states in order to evaluate consistently both the absorption band shape and the resonant Raman-scattering spectra for all the incident and scattered light polarizations and frequencies ω_L. We show results for Raman scattering in resonance with the F band in CsF in Figs. 1–4 for the different incident laser light wavelengths λ_L as given in the figures. These are obtained by using Eqs. (4), (6), (14), (21), and (29). The projected densities of phonon states are shown in Fig. 5. They have been calculated by

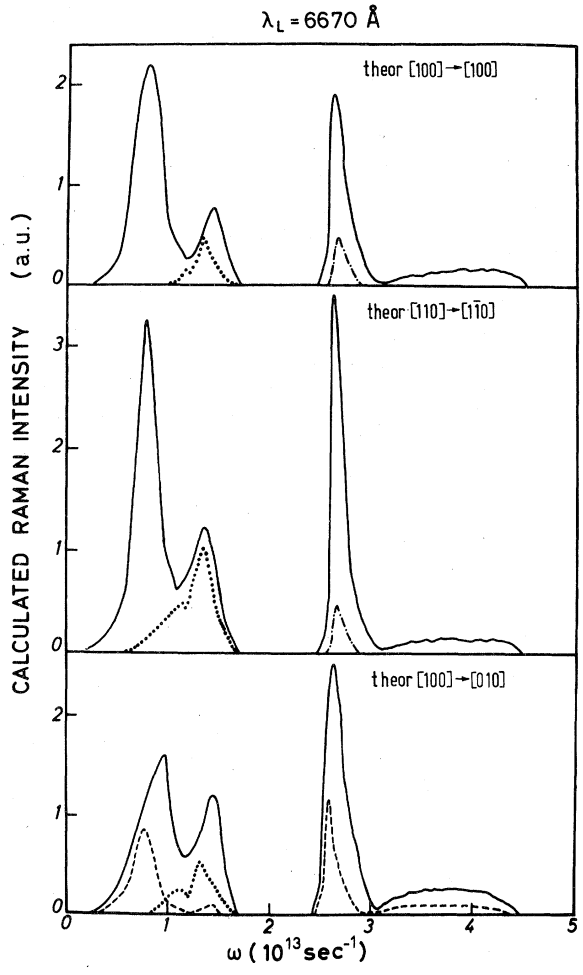

FIG. 3. Theoretical differential first-order Raman cross section for the indicated incident and scattered light polarizations and for $\lambda_L = 6670$ Å. The significance of the different curves is explained in the text.

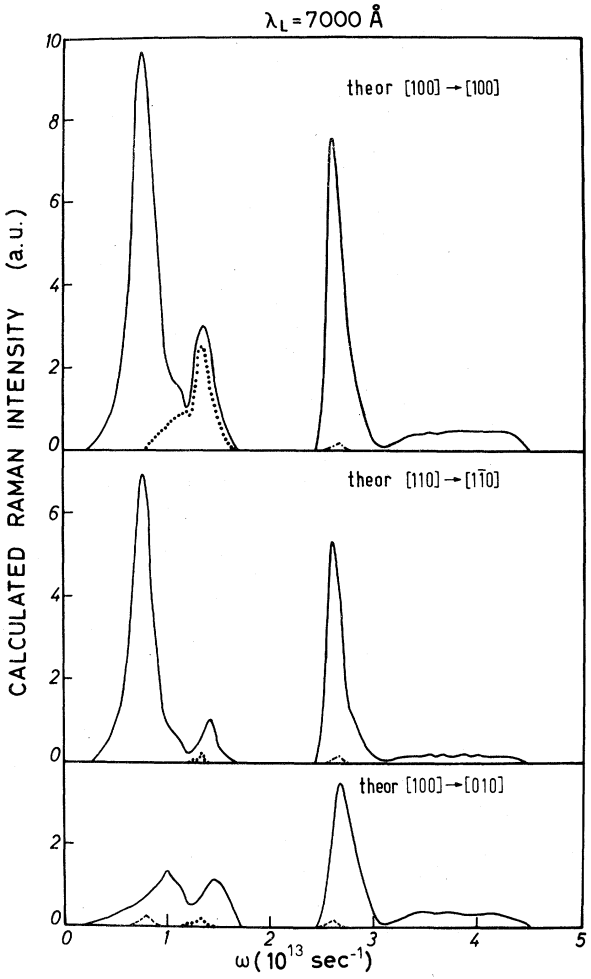

FIG. 4. Same as Fig. 3 for $\lambda_L = 7000$ Å.

using the breathing shell model[14] for the lattice dynamics of the CsF pure crystal with the parameters obtained in Ref. 15 from the best fit of the dispersion curves obtained using this model. We have considered only a change in the central force constant between the defect and the (NN) ions $\lambda_{cf} = -0.5f$*. Then only $\rho_{11}(\Gamma_1^+, \omega^2)$ and $\rho_{11}(\Gamma_3^+, \omega^2)$ entering Eq. (26) are evaluated as perturbed projected densities of phonon states, all the other ones entering that equation being taken as unperturbed projected densities of phonon states. The (NNN) densities of phonon states have been evaluated by using the expressions given in the Appendix of Ref. 16. The values of α_i entering Eq. (26), determined by the best fit found for the theoretical Raman spectra of Fig. 1, are 0.35, 0.50, and 1 for $i = 1, 3$, and 5, respectively. Moreover, we have used the values of A_i found in Ref. 7 from the best fit of the absorption band shape.

In the figures we have shown explicitly the main contributions from the various projected densities

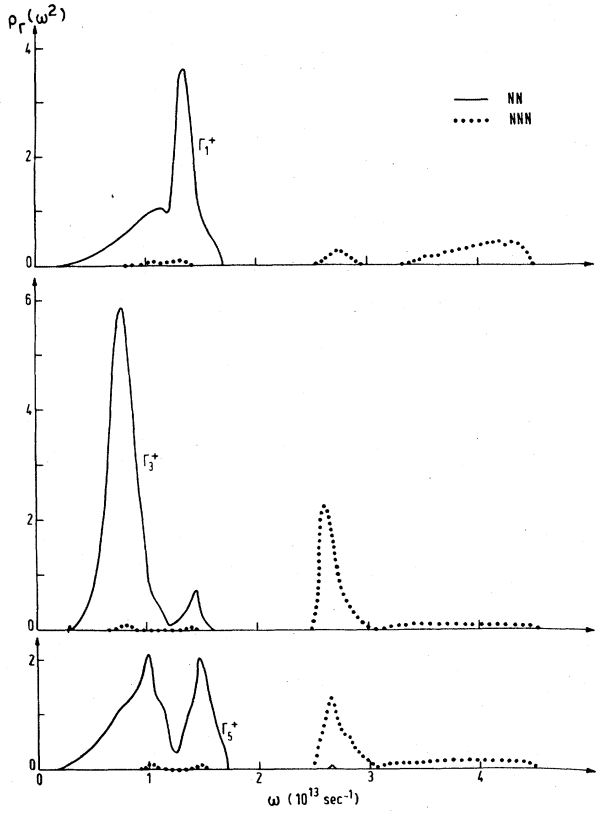

FIG. 5. The NN and NNN densities of phonon states used in order to evaluate the differential Raman cross sections shown in Figs. 1–4.

of states that determine the more important changes in the Raman spectra. In each figure the differential first-order Raman cross section (full line) is shown for the quoted incident and scattered light polarizations. The dotted (· · ·), dashed (---), and dash-dotted (-· -·) lines represent the contributions coming from the Γ_1^+, Γ_3^+, and Γ_5^+ phonon densities, respectively. When it is not specified otherwise, the differential Raman-scattering cross section for every polarization is determined by the densities of phonon states following the usual selection rules. When in a specific phonon frequency region a partial contribution coming from a particular Γ_i density of phonon states is shown, the differential first-order Raman-scattering cross section is determined by the sum of this partial contribution and the remaining contribution from the other Γ_j densities of phonon states ($j \neq i$). These other Γ_j phonon densities are the same as one obtains with the usual selection rules. As is possible to see from Figs. 1 and 2, the theoretical curves are in good agreement with the experimental data[1] obtained with the laser wavelengths $\lambda_L = 6100$ and 6400 Å, mainly in the spectral region where the NN and the NNN projected densities of phonon states give the most important contributions. Above all, we note the experimentally observed changes in the Raman spectra for the two different λ_L are consistent with those found theoretically, principally in the frequency region where $\rho_{22}(\Gamma_3^+, \omega^2)$ and $\rho_{22}(\Gamma_5^+, \omega^2)$ have the maximum ($\omega = 2.60 \times 10^{13}$ and 2.65×10^{13} sec^{-1}, respectively).

From Figs. 1 and 4 ($\lambda_L = 6100$ and 7000 Å, respectively) it is possible to see that the Raman-scattering spectra are largely determined by a superposition of the NN and the NNN projected densities of phonon states according to the usual selection rules. Moreover, we note that the most important feature of the spectra for $\lambda_L = 6400$ Å (Fig. 2) and $\lambda_L = 6670$ Å (Fig. 3) is determined by the change (with respect to Figs. 1 and 4) of the intensity of the peak at the transverse optical phonon frequencies [the maximum in the $\rho_{22}(\Gamma_3^+, \omega^2)$ and in the $\rho_{22}(\Gamma_5^+, \omega^2)$] with respect to the acoustical frequency region (determined by the NN projected densities of phonon states). These changes are explained theoretically by the contributions of the $\rho_{22}(\Gamma_3^+, \omega^2)$ in the $[100] \rightarrow [010]$ polarized scattering spectrum and of the $\rho_{22}(\Gamma_5^+, \omega^2)$ in the $[100] \rightarrow [100]$ and $[110] \rightarrow [1\bar{1}0]$ polarized scatterings spectra. The evaluated enhancement of the peaks at $\omega = 2.60 \times 10^{13}$ and 2.65×10^{13} sec^{-1} agrees quite well with the experimental data available for $\lambda_L = 6400$ Å (see Fig. 2). We note that the unusual contributions of the $\rho_{11}(\Gamma, \omega^2)$ and $\rho_{22}(\Gamma, \omega^2)$ for $\Gamma = \Gamma_1^+$, Γ_3^+, Γ_5^+ in the $[110] \rightarrow [1\bar{1}0]$ and $[100] \rightarrow [010]$ polarized scatterings prove that the Γ_4^+ Raman tensor component gives and important contribution to these polarized resonant scattering processes. Furthermore, for $\lambda_L = 6670$ Å the evaluations foresee an enhancement of the $\rho_{22}(\Gamma_3^+, \omega^2)$ mainly in the $[100] \rightarrow [100]$ and $[110] \rightarrow [1\bar{1}0]$ polarized spectra due to the resonance condition with that particular frequency of the absorption band. Unfortunately, the experimental data for $\lambda_L = 6670$ and 7000 Å are not available and we cannot check the theoretical predictions presented in Figs. 3 and 4. Moreover, in the theoretical differential Raman cross sections for $\lambda_L = 6100$ and 6400 Å, only the contributions coming from the F band are included, so that all the effects from the resonance condition with the K band are not accounted for here. These additional contributions may account for the part of the Raman-scattering spectra in the longitudinal optical phonon frequencies that the present evaluations, considering only the NN and the NNN densities of phonon states, cannot explain.

A different situation with respect to the CsF case is found in the resonant Raman spectra of the F center in CsBr.[5] In fact, there the most impor-

tant changes in the polarized spectra obtained by considering different λ_L are mainly determined by the various contributions of the Γ_1^+ projected density of phonon states to all the polarized scatterings. In those evaluations we have considered only the NN projected densities of phonon states. From Ref. 5 it is possible to see that the agreement between the experimental evaluations is quite good in the frequency region of the spectra where the NN densities of phonon states give the most important contribution for all the λ_L considered. Above all, we note that the most important feature of the scattering spectra in that phonon frequency region, determined by the change with λ_L of the intensity of the $\rho(\Gamma_1^+, \omega^2)$ contribution to the different polarized spectra, is completely explained by the theoretical calculations (see Figs. 2–5 of Ref. 5). We note, for instance, that for λ_L = 625 nm (Fig. 3 of Ref. 5) $\rho(\Gamma_1^+, \omega^2)$ gives the most important contribution in the $[110] \rightarrow [1\bar{1}0]$ and $[100] \rightarrow [010]$ polarized spectra. In addition, from Fig. 5 of Ref. 5 we see that the contribution of $\rho(\Gamma_1^+, \omega^2)$ for these polarized scattering spectra becomes dominant with respect to the usual one (in the $[100] \rightarrow [100]$ polarized scattering) when the incident light frequency ranges from 610 to 630 nm, reaching its maximum when $\lambda_L = 625$ nm. From the selection rules given in Eq. (3) of Sec. II and the discussion given there, it follows that in the same frequency range the Γ_4^+ Raman tensor component is the dominant one in determining the scattering processes, reaching the maximum of intensity for $\lambda_L = 625$ nm.

As noted before, in the experimental spectra for the CsF case and for the CsBr case,[1] the part of the first-order scattering spectra near the longitudinal optical-phonon frequency ω_l cannot be explained by the correlations of the ion displacements and by the electron-phonon interactions that we have considered here and in Ref. 5. Furthermore, the intensity of this part of the spectra increases as λ_L begins to be in resonance with the K band. From lattice-dynamical evaluations,[17] this feature in the first-order scattering spectra has been shown to be due to the contribution of the perturbed projected densities of phonon states determined from the correlations of the displacements of the ions beyond the next-nearest-neighbors of the F center. In fact, the wave functions of the excited states that contribute to the K band are extended over many neighbors of the F center. Then the electron-phonon interactions in these excited states are substantially long range and the autocorrelations of all the ion displacements of the crystal space where the electron-phonon interactions act must be considered when λ_L is in resonance with the K band.

Nevertheless we note that when λ_L is in resonance with the K band, the selection rules given In Sec. II of the present paper are still valid whenever the excited states involved in determining the K band have a spin-orbit interaction coupling different from zero. Then the only changes in the theoretical evaluations that emerge by including the additional K-band contribution are determined by the consideration of the many-neighbor ion-displacement correlations and by the inclusion in the cross sections given in Eq. (4) of the functions analogous to the $S_{\alpha\alpha'}(\omega_L)$ considered here, which take into account the contribution of the K-band scattering response functions.

V. CONCLUSIONS

We can summarize the main results presented here as follows: We have shown that new selection rules apply when Raman scattering is in resonance with a transition from a spin-degenerate ground state to an excited state for which the spin-orbit interaction is nonvanishing. In connection with these new selection rules we have also shown that the antisymmetric (transforming as Γ_4^+) component of the Raman tensor becomes effective in determining the scattering, reaching the maximum intensity for some resonant light frequency. We have applied the theory to the F center in CsF and have compared these results with those obtained for CsBr. We have found that $\rho(\Gamma_3^+, \omega^2)$ gives the most important contribution in all the polarized resonant Raman spectra in CsF. This differs from the situation in CsBr where it is $\rho(\Gamma_1^+, \omega^2)$ that gives the most important contribution in all the polarized spectra. Moreover, we have shown that in the case of CsBr the Γ_4^+ component of the Raman tensor determines the intensity of the $\rho(\Gamma_1^+, \omega^2)$ contribution in the $[110] \rightarrow [1\bar{1}0]$ and $[100] \rightarrow [010]$ polarized spectra for the different incident laser light frequencies. In the case of CsF, however, the Γ_4^+ component of the Raman tensor is responsible for the unusual contribution of the densities of phonon states transforming as Γ_1^+, Γ_3^+, Γ_5^+ to the $[110] \rightarrow [1\bar{1}0]$ and $[100] \rightarrow [010]$ polarized spectra.

ACKNOWLEDGMENTS

The author would like to thank Marilyn F. Bishop for critically reading the manuscript. This research was supported in part by the Materials Research Laboratory Program of the National Science Foundation.

*Permanent address: Instituto di Fisica, Università di Milano and Gruppo Nazionale di Struttura della Materia del Consiglio Nazionale delle Ricerche, via Celoria 16, Milano, Italy.

[1]J. P. Buisson, A. Sadoc, L. Taurel, M. Billardon, and R. C. C. Leite, Phys. Status Solidi B 78, 779 (1976); J. P. Buisson, S. Lefrant, M. Ghomi, and L. Taurel, in *Proceedings of the International Conference on Lattice Dynamics, Paris, 1977,* edited by M. Balkanski (Flammarion, Paris, 1978), p. 223; J. P. Buisson, S. Lefrant, M. Ghomi, L. Taurel, and J. P. Chapelle, Proceedings of International Conference on Defects in Insulating Crystals, Gatlinburg, 1977 (unpublished); Phys. Rev. B 18, 885 (1978). From the experimental data from CsF, see, in particular, J. P. Buisson, and S. Lefrant, C. R. Acad. Sci. Ser. B 285, 207 (1977); Phys. Status Solidi B 86, 493 (1978).

[2]Nguyen Xuan Xinh, A. A. Maradudin, and R. A. Coldwell Horsfall, J. Phys. (Paris) 26, 717 (1965).

[3]E. Mulazzi and N. Terzi, Solid State Commun. 18, 721 (1976).

[4]E. Mulazzi and M. F. Bishop, J. Phys. (Paris) 37, C7-109 (1976). In the [100]→ [100] scattering cross section given in Eq. (5b) of this reference, the $\rho(\Gamma_3^+, \omega^2)$ contribution has been evaluated without considering the interference effects between the $S_{22}(\omega)$ function and the $[S_{12}(\omega)+S_{21}(\omega)]$ function.

[5]E. Mulazzi and J. P. Buisson, in *Proceedings of the International Conference on Lattice Dynamics, Paris, 1977,* edited by M. Balkanski (Flammarion, Paris, 1978, p. 220. In this paper there is a typographical error in Eq. (3) which should read $(S_{11}+2S_{22})$.

[6]E. Mulazzi and M. F. Bishop, Solid State Commun. 19, 39 (1976).

[7]E. Mulazzi, Phys. Rev. B 18, 7109 (1978).

[8]G. Benedek, I. Pollini, and G. Spinolo, in *Proceedings of the International Conference on Lattice Dynamics, Paris, 1977,* edited by M. Balkanski (Flammarion, Paris, 1978), p. 68.

[9]R. Merlin, R. Zeyher, and G. Guntherodt, Phys. Rev. Lett. 39, 1215 (1977).

[10]E. Mulazzi and N. Terzi, Phys. Rev. B 19, 2332 (1979).

[11]See, for instance, V. Heine, *Group Theory in Quantum Mechanics* (Pergamon, London, 1960).

[12]The electron-phonon interaction coupling $C(\Gamma_1^+)$ is determined by the difference between the coupling of the Γ_1^+ electron-phonon interaction in the Γ_8^- and Γ_6^- states and the coupling of the hole-phonon interaction in the Γ_6^+ state.

[13]Since in the present paper we are only interested in showing the interplay of the different contributions of the $\rho(\Gamma, \omega^2)$ for $\Gamma = \Gamma_1^+$, Γ_3^+, Γ_5^+ in the different polarized first-order resonant Raman scattering spectra, this is a sufficiently good approximation. In fact, as we have found in the evaluations of the absorption *F* band in CsF, the inclusion of the A_i' terms proportional to t^3 [in the $\varphi(\Gamma, t)$ expansion] gives only a better agreement between the calculated and the experimental data, but it does not change the values of $C(\Gamma_i^+)$ and the positions of structures due to the spin orbit and Jahn-Teller interactions.

[14]U. Schröder, Solid State Commun. 4, 347 (1966).

[15]S. Rolandson, Phys. Status Solidi B 52, 643 (1972).

[16]G. Benedek and E. Mulazzi, Phys. Rev. 179, 906 (1969).

[17]D. Robbins and J. B. Page, Phys. Rev. Lett. 38, 365 (1977).